

RESEARCH ARTICLE

10.1002/2017JA024956

Key Points:

- Occurrence of simultaneous F_3 layers at equator and E_{sb} layers at low latitude but suppression of EPBs in the dusk sector in the recovery phase of a magnetic storm
- Intense E_{sb} layers at low latitude when EPBs are suppressed on the storm day but are weak when EPBs occur on quiet days
- The altitude/latitude variation of DD electric fields in the sunset sector may be responsible for these results

Correspondence to:

S. Sripathi,
ssripathi.iig@gmail.com

Citation:

Sripathi, S., Banola, S., Emperumal, K., Suneel Kumar, B., & Radicella, S. M. (2018). The role of storm time electrodynamic in suppressing the equatorial plasma bubble development in the recovery phase of a geomagnetic storm. *Journal of Geophysical Research: Space Physics*, 123, 2336–2350. <https://doi.org/10.1002/2017JA024956>

Received 1 NOV 2017

Accepted 27 FEB 2018

Accepted article online 5 MAR 2018

Published online 25 MAR 2018

The Role of Storm Time Electrodynamic in Suppressing the Equatorial Plasma Bubble Development in the Recovery Phase of a Geomagnetic Storm

S. Sripathi^{1,2} , S. Banola¹, K. Emperumal³, B. Suneel Kumar⁴, and Sandro M. Radicella⁵ 

¹Indian Institute of Geomagnetism, New Bombay, India, ²Also at ICTP, Trieste, Italy, ³Equatorial Geophysical Research Laboratory, Indian Institute of Geomagnetism, Tirunelveli, India, ⁴TIFR Balloon Launch Facility, Hyderabad, India, ⁵International Centre for Theoretical Physics, Trieste, Italy

Abstract We investigate the role of storm time electrodynamic in suppressing the equatorial plasma bubble (EPB) development using multi-instruments over India during a moderate geomagnetic storm that occurred on 2 October 2013 where Dst minimum reached ~ -80 nT. This storm produced unique signatures in the equatorial ionosphere such that equatorial electrojet strength showed signatures of an abrupt increase of its strength to 150 nT and occurrence of episodes of counter electrojet events. During the main phase of the storm, the interplanetary magnetic field Bz is well correlated with the variations in the equatorial electrojet/counter electrojet suggesting the role of undershielding/overshielding electric fields of magnetospheric origin. Further, observations showed the presence of strong F_3 layers at multiple times at multiple stations due to undershielding electric field. Interestingly, we observed simultaneous presence of F_3 layers and suppression of EPBs in the dusk sector during the recovery phase. While strong EPBs were observed before and after the day of the geomagnetic storm, suppression of the EPBs on the storm day during “spread F season” is intriguing. Our further analysis using low-latitude station, Hyderabad, during the time of prereversal enhancement suggests that intense E_{sb} layers were observed on the storm day but were absent/weak on quiet days. Based on these results, we suggest that the altitude/latitude variation of disturbance dynamo electric fields/disturbance winds may be responsible for simultaneous detection of F_3 layers, occurrence of low-latitude E_s layers, and suppression of EPBs during the storm day along the sunset terminator.

1. Introduction

Equatorial ionosphere favors variety of electrodynamic processes both during quiet and disturbed periods owing to its unique geometry where geomagnetic fields are nearly horizontal (e.g., Fejer & Kelley, 1980). The primary eastward zonal electric field in the presence of a horizontal geomagnetic field (in the magnetic north-south direction) over the magnetic equator produces vertical upward $E \times B$ drift during daytime through the E region dynamo process. This results in drifting of the F layer to higher altitudes and produces anomaly crests on either sides of the magnetic equator. However, since E region dynamo reduces in the postsunset sector due to reduction of E region density, F region dynamo dominates and produces enhanced zonal electric fields in the evening sector to produce prereversal enhancement (PRE) in the upward vertical drift that raises the F layer to higher altitudes. These vertical drifts have large variability or decrease with altitude in the evening times so that PRE is dominant at equator. This setup, under favorable conditions, generates plasma irregularities best known as equatorial spread F (ESF) irregularities or equatorial plasma bubbles (EPBs). When these irregularities propagate upward, they evolve nonlinearly through cascading process and produces wide range of plasma irregularities ranging from few tens of centimeters to few hundreds of kilometers. The generation mechanism for these plasma irregularities is believed to be due to the Rayleigh-Taylor (RT) instability. These plasma irregularities can be detected as plasma plumes or plasma bubbles by ionospheric radars, EPBs in optical airglow, scintillations in transionospheric radio signal, and radio biteouts in Global Positioning System (GPS) receivers (e.g., Fejer & Kelley, 1980). It is also known that the equatorial ionosphere is electrodynamic coupled with high-latitude ionosphere during major geomagnetic storms and produces large deviations from quiet time variations (e.g., Abdu et al., 1995, 1998; Abdu, 1997; Fejer, 1997; Kikuchi et al., 1996; Ramsingh et al., 2015). Based on several simultaneous geomagnetic and ionospheric observations in the past, it is suggested that the geomagnetic storms play crucial role in either suppressing or enhancing the generation of EPBs depending upon the onset time of the storm (e.g., Aarons, 1991;

Abdu, Batista, et al., 2003; Huang et al., 2005; Sastri et al., 2002; Tulasi Ram et al., 2008). In addition, other signatures of geomagnetic storm disturbances that are frequently observed at low latitudes during major storms are westward thermospheric winds, disappearance of equatorial E_{s-q} layers, episodes of equatorial electrojet (EEJ) and counter electrojet (CEJ) currents, and occurrence of F_3 layers (e.g., Abdu et al., 1995; Balan & Bailey, 1995; Chandra & Rastogi, 1974).

It is known that, during geomagnetic storms, sudden southward turning of the interplanetary magnetic field (IMF) Bz from an existing northward configuration produces a dawn to dusk convection electric field (e.g., Huang et al., 2002; Kikuchi et al., 1996; Somayajulu et al., 1987). This in turn produces eastward (westward) electric fields during daytime (nighttime) due to undershielding. However, under northward IMF Bz condition, westward (eastward) electric fields dominates during daytime (nighttime) due to overshielding (Kelley et al., 1979; Kikuchi et al., 1996). As the undershielding electric field is active in the main phase of the storm, it penetrates directly to the equatorial and low latitudes as prompt penetration (PP) electric field. In addition, other types of geomagnetic disturbances such as disturbance winds and disturbance dynamo (DD) electric fields that are generated at high latitudes due to Joule heating also affect the dynamics of the low-latitude ionosphere (e.g., Blanc & Richmond, 1980; Sastri, 1988). Here it may be mentioned that even though both direct and delayed storm time disturbances can impact the equatorial and low-latitude ionosphere, significant differences arise between these two types due to differences in their direction of propagation, polarity, time of arrival, and generation mechanisms. While the low latitudes are instantly affected by the PP electric fields, disturbance dynamo electric fields (DDEFs) impact the low latitudes rather slowly with typically of 3 h to few days (e.g., Blanc & Richmond, 1980). The Joule heating generated during geomagnetic storm produces large-scale atmospheric wind circulation that transports neutral densities to low latitudes by the process of upwellings at high latitudes, downwellings at low latitudes, and disturbance winds (e.g., Lee et al., 2002; Lei et al., 2008; Nava et al., 2016). Two mechanisms are believed to cause DDEFs to propagate to low latitudes. While, in the first process, the DD at midlatitude produces electric fields and then penetrates to equatorial latitudes, in the second process, DD at equatorial latitudes produces electric fields locally. The second process is slower than first process. These electric fields are usually known as DDEF, and they produce disturbances at equatorial and low latitudes (e.g., Fejer, 1997). Significant progress has been made in the past to identify the influence of the geomagnetic storms on the generation/suppression of ESF irregularities (e.g., Aarons, 1991; Martinis et al., 2005; Rastogi et al., 1981). Now it is generally agreed that while storms trigger the postmidnight ESF (e.g., Dabas et al., 1989; DasGupta et al., 1985), suppression of ESF was reported during the postsunset period (e.g., Alex & Rastogi, 1986). Other studies suggest that postsunset ESF is generated during non-ESF season, while it is suppressed during ESF season (e.g., Aarons, 1991; Becker-Guedes et al., 2004; Rastogi et al., 1981). Abdu et al. (2009, 2014) presented some results of the response of the equatorial ionosphere to PP electric fields in the evening sector where they showed that the evening upward vertical drifts can completely be suppressed by overshielding electric field of westward polarity arising from overshielding condition results in inhibition of ESF irregularities. However, in contrast, the undershielding PP electric field of eastward polarity is found to enhance the upward vertical drift to produce ESF irregularities.

It is known that low-latitude E region conductivity around sunset terminator plays significant role in causing the ESF variability in terms of flux tube-integrated conductivities (e.g., Abdu, MacDougall, et al., 2003, Abdu et al., 2013; Bhattacharyya, 2004; Stephan et al., 2002). It is also known that E_s layers are affected by the geomagnetic storms (e.g., Chandra & Rastogi, 1974; Rastogi, 1974). Abdu, MacDougall, et al. (2003) have thoroughly investigated the evening PRE enhancement and its relation to E_s layer formation in the evening hours over Fortaleza, a low-latitude station in Brazil. Their result suggests that larger PRE amplitudes are found to disrupt the E_s layers, whereas under smaller PRE amplitudes such disruption does not occur. They suggested that the E and F region coupling around sunset could affect strongly the linkage between PRE drifts and E_s layer disruption or formation. Using Sriharikota ionosonde, Joshi, Patra, and Rao (2013) and Joshi, Patra, Pant, and Rao (2013) have examined the role of quiet time low-latitude E_s layer activity on the generation of ESF irregularities around the sunset terminator over India. They suggested that E_s layers play significant role in the occurrence of ESF irregularities in the sunset terminator depending upon the type of E_s layer. However, they did not investigate the role of geomagnetic storms on the development of low-latitude E_s layers and its impact on the occurrence or nonoccurrence of ESF irregularities.

Table 1
List of Stations Used in the Present Investigations

Location	Name of the instrument	Geo. latitude	Geo. longitude	Geomag. latitude
Tirunelveli (TIR)	CADI and GPS receiver	8.73°N	77.7°E	0.23°N
Hyderabad (HYD)	CADI	17.36°N	78.47°E	8.76°N
Allahabad (ALD)	CADI	25.43°N	81.84°E	16.48°N
West Sumatra, Indonesia	EAR	0.2°S	100.32°E	Dip: 10.36°S

Note. CADI = Canadian Advanced Digital Ionosonde; GPS = Global Positioning System; EAR = equatorial atmospheric radar.

While many reports have showed the generation/suppression of EPBs linked to storms, there is no report available that showed the suppression of EPBs simultaneously in the presence of evening hour F_3 layers. As suppression of EPBs is caused by downward drift and production of F_3 layers due to upward drift, presence of both signatures simultaneously in the present storm suggests significant differences in their electrodynamic processes. Sreeja et al. (2009) have studied the occurrence of F_3 layers over Trivandrum during geomagnetic storms at dawn and dusk sectors and associated them to the sudden changes in the IMF Bz. In the present study, we examine the ionospheric response over Indian region to one of the moderate geomagnetic storms that occurred on 2 October 2013 following the eruption of a huge cloud of charged particles from the Sun propelled by a large erupting magnetic filament that was very close to active region 1850 on 29–30 September 2013 (night). The coronal mass ejections with solar wind speed of ~650 km/s that hit the Earth’s magnetosphere at around 22:00 EDT (02:00 UT on 2 October 2013) on 1 October resulted in a moderate geomagnetic storm with minimum Dst value of –80 nT on the ground. The $\sum Kp$ indexes are 9, 39, and 7–, while Ap indexes are 4, 58, and 4, respectively, for 1–3 October 2013. The aim of this paper is to understand the role of storm time electrodynamics in causing the day-to-day variability of the equatorial plasma irregularities or plasma bubbles under such moderate geomagnetic storms.

2. Details of the Instruments and Data Sets

Multistation observations of Canadian Advanced Digital Ionosonde that are located at Tirunelveli, Hyderabad, and Allahabad over India are manually scaled to study its response to the moderate geomagnetic storm of 2 October 2013. In addition to the storm day, we also considered two quiet days, namely, 1 and 3 October 2013, to examine the storm day variations with respect to the quiet days. It may be mentioned that since Ap is only 4 on both these days, we consider that they are geomagnetically quiet days. It may be mentioned that Tirunelveli is located at dip equator, while Hyderabad and Allahabad are located at southern and northern edge of the ionization crest region over Indian region. The ionograms at Tirunelveli/Hyderabad are obtained at every 10 min; however, it is obtained at every 15 min in Allahabad. We also obtained geomagnetic activity indices such as Kp, auroral index (AE), and symmetric ring current (SYM-H) (i.e., high resolution of Dst index) during the same period from World Data Center, Kyoto university, Japan. Simultaneously, we also collected GPS receiver data at Tirunelveli. From the GPS receiver, we obtained L-band scintillations as well as slant TEC (total electron content) (STEC). From the STEC, vertical TEC (VTEC) is obtained through the mapping function. Mathematically, it can be written as $VTEC = STEC \times \cos(\chi)$ where $\chi = \sin^{-1} \left(Re * \frac{\cos(\alpha)}{(Re+h)} \right)$, where α is elevation angle at ionospheric piercing point at the altitude, $h = 350$ km and $Re = 6,378$ km. In addition, 1 min ∇H values (representative of EEJ currents) of Earth’s magnetic field as calculated by measuring the H component variations of the Earth’s magnetic field at Tirunelveli (equator) and subtracting the same H component variations, which is measured at Alibag (low latitude), respectively, after accounting for baseline adjustments at local midnight. We also utilize radar maps from equatorial atmospheric radar located at West Sumatra, Indonesia. More details about this system can be found in an article by Fukao et al. (2004). Table 1 summarizes the list of instruments and their locations that are used in the present study.

3. Observations and Results

Figures 1a–1c show the high-resolution (~16 s) observations of time-shifted IMF Bz variations in geocentric solar magnetospheric coordinates as obtained from the ACE satellite at L1 point along with AE index and

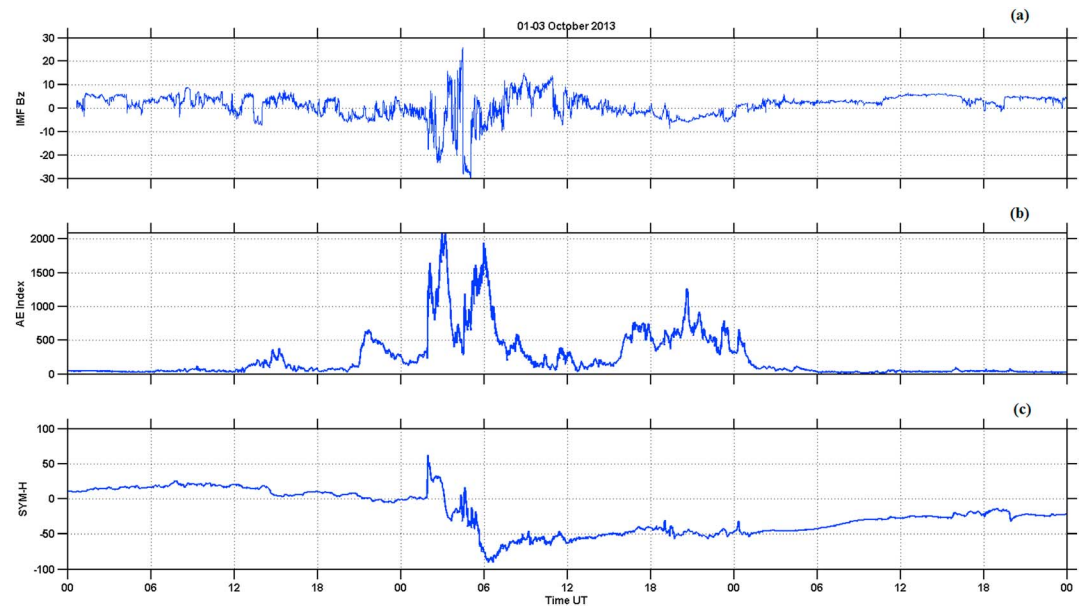


Figure 1. The temporal variation of (a) interplanetary magnetic field Bz (nT), (b) AE index, and (c) SYM-H during 1–3 October 2013 (storm period).

SYM-H, respectively, for the period of 1–3 October 2013. From the SYM-H observations, it is evident that on 2 October 2013 geomagnetic storm is commenced with a storm sudden commencement at the time of 02:00 UT. The IMF Bz sharply fluctuated between north/southward turning during 02:00 to 05:00 UT on 2 October, with two negative/positive excursions of 20 and 30 nT at 02:00 and 04:00 UT, respectively. Then IMF Bz turned northward at 07:00 UT and remained northward until 10:00 UT. After 12:00 UT, IMF Bz became small. On the other hand, AE initially had normal values on 1 October 2013 except at 15:00 UT and 21:00 UT where AE increased to 300 nT and 500 nT for a brief period. However, AE increased to $\sim 2,000$ nT at 02:00 UT on 2 October 2013. Immediately, it fell down to 300 nT at 04:00 UT. Later, AE sharply increased to $\sim 1,800$ nT at 06:00 UT for a brief period before it sharply fell down to ~ 500 nT on the same day. Then it was fluctuating at about 100–200 nT until 13:00 UT and went to ~ 500 nT for about 3 h during 15:00 to 18:00 UT, which continued with the same level, however, with some spiky structures at 21:00, 22:00, and 23:30 UT on 2 October 2013 and at 01:30 UT on the next day (3 October 2013). Later, AE became normal with negligible fluctuations. On the other hand, SYM-H was steadily varying on 1 October 2013 with mean of ~ 10 nT. At 22:00 UT, the SYM-H started reducing its value to almost 0. This is continued until 02:00 UT on 2 October 2013. Storm sudden commencement started at 02:00 UT as can be seen in the figure where SYM-H went up to ~ 60 nT for a brief period and fell stepwise before it went into negative at 03:00 UT on 2 October 2013. As time progresses, SYM-H decreased in its strength with small fluctuations but its mean could not go to positive excursion until 04:00 UT. Following that, SYM-H went down and reached -80 nT at $\sim 06:20$ UT on 2 October 2013 and then it started recovering gradually. Based on Gonzalez et al. (1994), this storm is a moderate geomagnetic storm. While Mao et al. (2015) and Lei et al. (2016) have examined the ionospheric response to this storm event over China with ground-based observations and modeling, we focus here on the ionospheric response in the dusk sector on 2 October 2013 by using ground-based ionosondes and GPS receiver observations over Indian sector.

To examine the temporal variations of F layer height at the time of PRE on quiet days and on storm day, we present the ionogram height analysis of the F layer at 4 MHz and its corresponding vertical drifts at Tirunelveli in Figures 2a and 2b. While Figure 2a shows the variations in the virtual height of the F layer, Figure 2b shows the corresponding vertical drift derived using rate of change of layer height. We show the h'F (km) at 4 MHz and corresponding drift variations only from the evening hours at 12:30 UT (18:00 IST) to next day early morning hours, that is, 00:30 UT on 1–3 October 2013, respectively. Red, blue, and black lines represent 2 October, 1 October, and 3 October, respectively. Accordingly, we can attribute the height variations of the F layer as

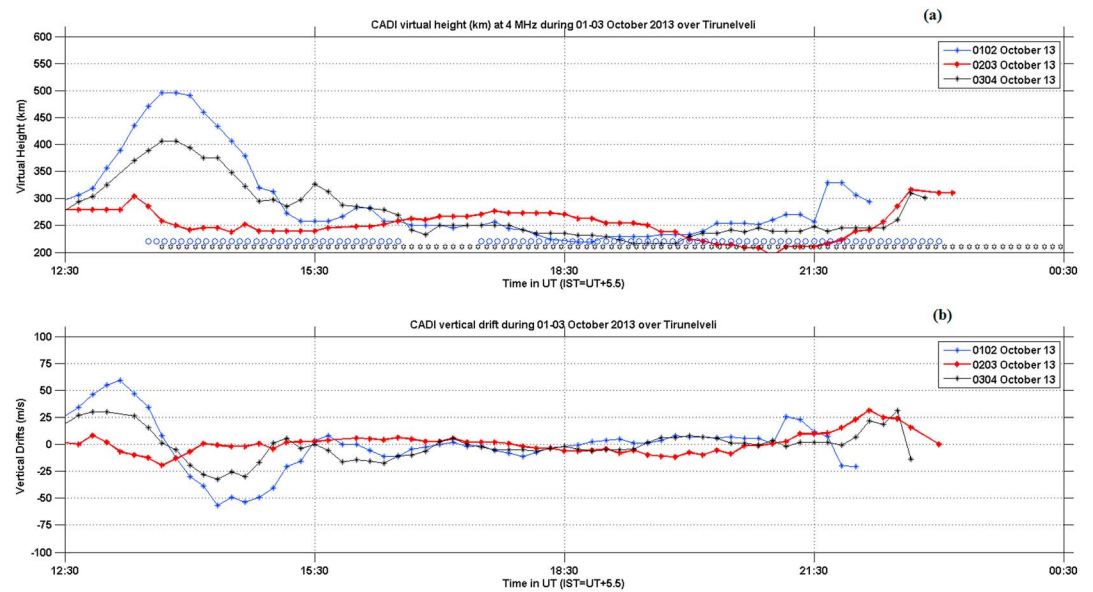


Figure 2. The (a) temporal variation of virtual height ($h'F$ (km)) scaled at 4 MHz and (b) corresponding vertical drifts in the postsunset sector on 1–3 October 2013 over Tirunelveli. Here blue, red, and black correspond to 1–3 October 2013, respectively. The spread F durations for 1 and 3 October 2013 are shown as blue circles and black hexagons in Figure 2a. CADI = Canadian Advanced Digital Ionosonde.

shown in the above figure to electrodynamic drift as shown in the Figure 2b after assuming that recombination effect is negligible. Here the durations of the spread F in Figure 2a are shown in blue circles and black hexagons for 1 and 3 October 2013, respectively. The figure suggests that there is no spread F on 2 October 2013 but spread F is present on other two quiet days. From the figure, it can also be seen that initially F layer height is steadily varied during two quiet days but on 2 October 2013 (storm day) the height is steady initially but bit higher after 13:30 UT for a brief period, which is different than other two days. But as time progresses, the F layer height increased gradually and reached ~ 490 km and ~ 420 km on 1 and 3 October 2013, respectively. While the F layer height on storm day is steady at ~ 275 km than other 2 days initially, as time progresses its height slowly reduced to ~ 240 km at 14:30 UT (20:00 IST) on 2 October 2013. Its height further started increasing after 16:30 UT (i.e., 22:00 IST) and reached a maximum of 275 km at 17:30 UT (23:00 IST). Later, it fell down to 200 km before it started again increasing during early morning hours (next day). On this storm day, no spread F is seen that contrasts with the other two quiet days where spread F is strong. The corresponding vertical drifts on these days also suggest that vertical drifts are higher on 1 October 2013 followed by 3 October 2013. But on storm day, the drifts show initially upward, but later it becomes downward with a maximum magnitude of -25 m/s. The drift became almost steady after 13:30 UT on storm day. This is in contrast to quiet days where the drifts showed initially upward with a maximum of 25 and 50 m/s at 13:00 UT on 1 and 3 October, respectively, but later at 14:00 UT it went down with similar magnitudes. After 15:00 UT, the drifts are steady with minor fluctuations on quiet days. Here it may be noted that there could be some errors in the estimation of vertical drifts using rate of change of $h'F$ (km) as recombination effects can become important when $h'F$ (km) goes below 300 km. However, it will not significantly alter the final results. To make the results more reliable, the temporal variation of $h'F$ (km) is also shown in Figure 2a. It may be mentioned that October falls in autumn equinox, which is considered to be strong spread F season over Indian region (e.g., Subbarao & Murthy, 1994). So decrease of F layer height and absence of spread F on storm day (2 October 2013) during spread F season is quite interesting. Simultaneously, we have recorded ionospheric L-band scintillations and GPS TEC using a GPS receiver at Tirunelveli, which also showed the TEC biteouts and L-band scintillations on 1 and 3 October 2013 but not on 2 October 2013 (storm day). These results are shown in Figures 3a–3c, which show the temporal variation of L-band scintillations on 1–3 October 2013, respectively. Up to now, we discussed only ionosonde spread F and GPS L-band scintillations. To confirm that EPBs were indeed present on 1 and 3 October but not on 2 October 2013, we examined the

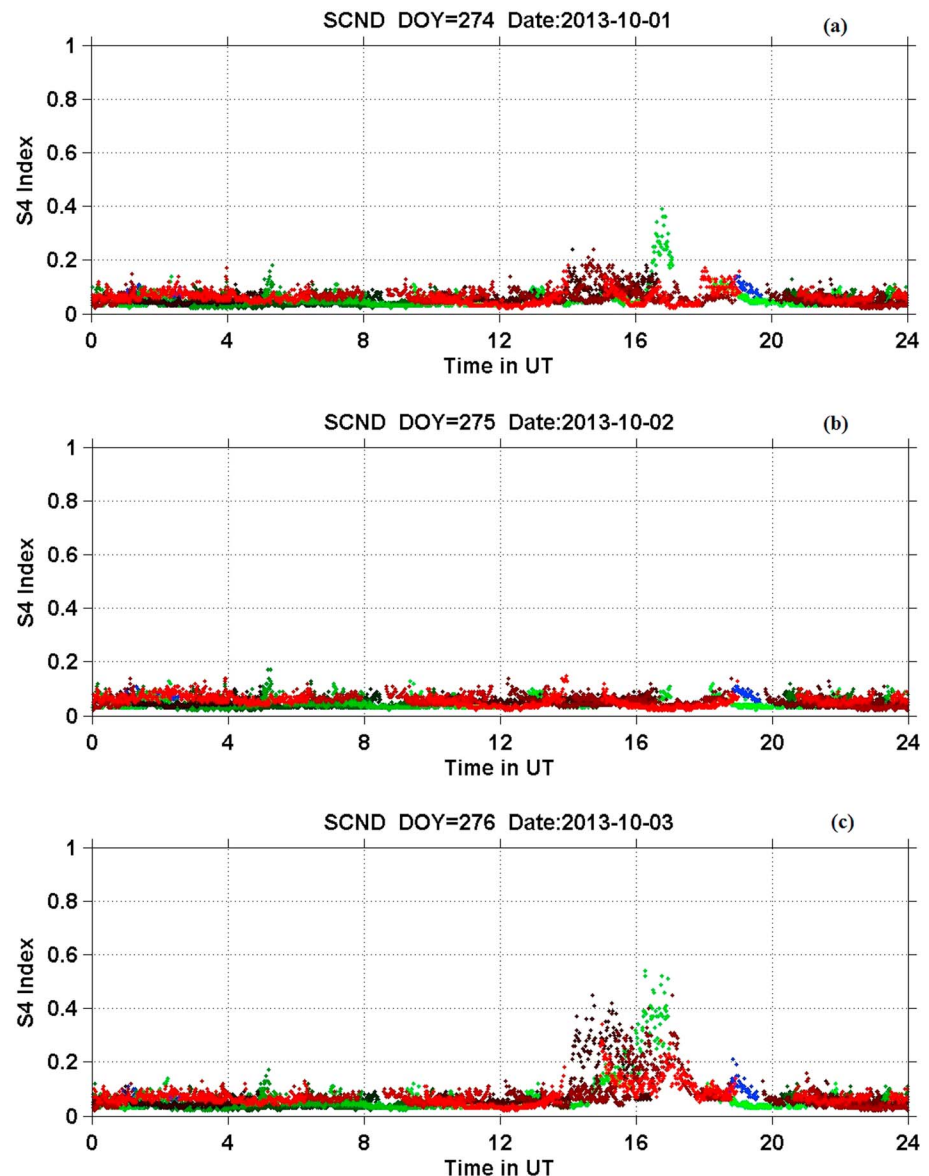


Figure 3. The temporal variation of nighttime Global Positioning System L-band scintillations over Tirunelvelion (a) 1 October 2013, (b) 2 October 2013, and (c) 3 October 2013. DOY = day of year.

equatorial atmospheric radar maps over Indonesia, which is $\sim 15^\circ$ east of India on these days. Figures 4a–4c show the radar signal-to-noise ratio as a function of time and altitude during 1–3 October 2013. In the x axis, both local time (bottom) and UT time (top) are shown. From the observations, it is evident that EPBs were indeed present on 1 and 3 October but not on 2 October 2013 (storm day). Some enhanced signal is present at few heights on 2 October 2013, which is nothing but noise. After midnight on 3 October, radar data are not available possibly due to nonoccurrence of radar echoes. So this confirms that we are actually observing plasma bubbles on other 2 days but not on storm day.

Here we present the response of the equatorial and low-latitude ionosphere to the current storm as investigated over Indian longitude using combination of EEJ strength and network of ionosondes located at Tirunelveli (TIR), Hyderabad (HYD), and Allahabad (ALD). Figures 5a–5c show the temporal variation of virtual height as scaled using isodensity at 4–10 MHz as obtained from Canadian Advanced Digital Ionosonde over (a) ALD, (b) HYD, and (c) TIR, respectively, during 00:00–18:00 UT (05:30–23:30 IST) on 2 October 2013, which is a storm day. In isodensity scaling, the height variations in the ionograms are recorded at fixed frequencies

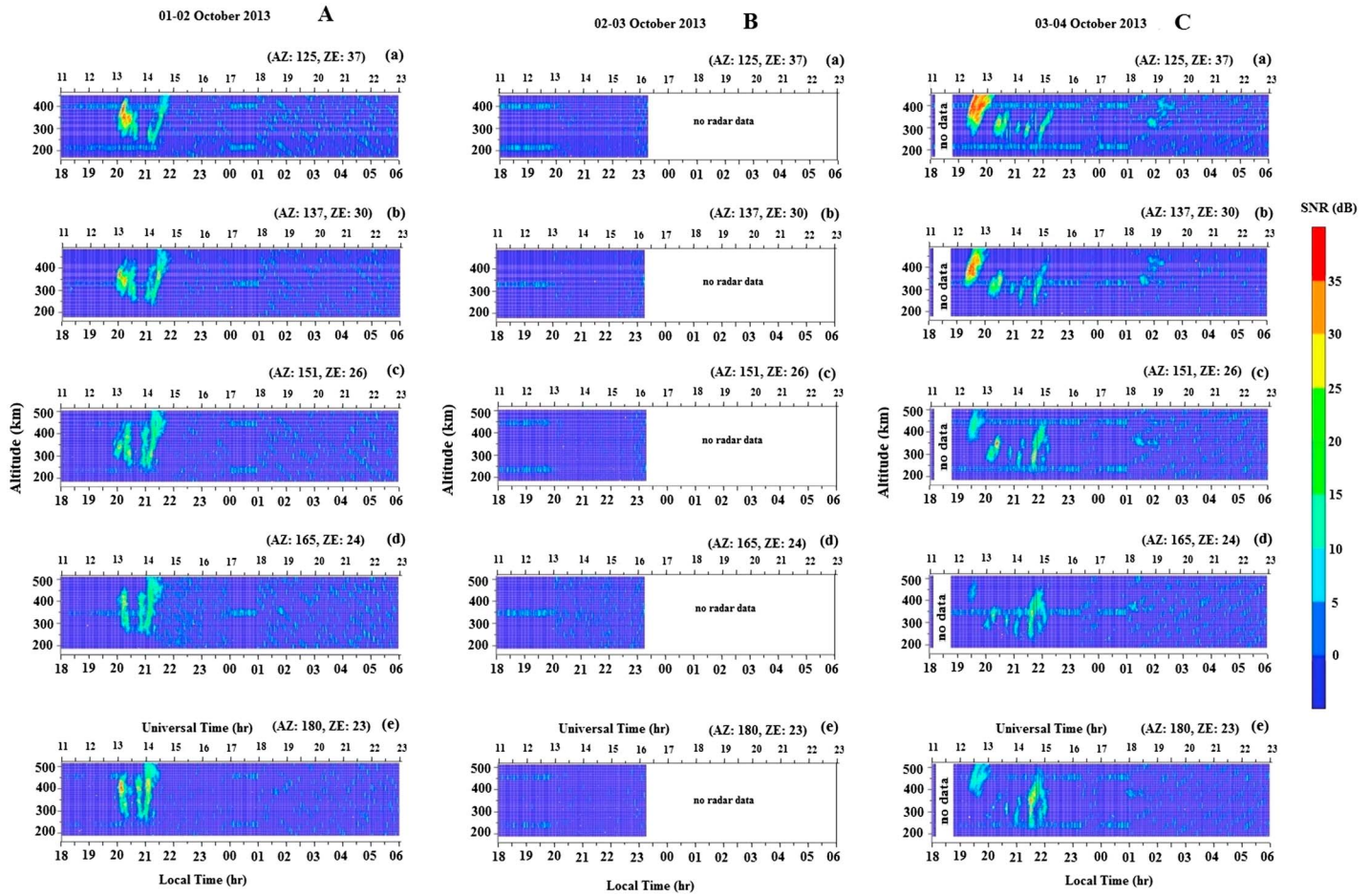


Figure 4. (A–C) The range-time-intensity maps obtained from equatorial atmospheric radar in west Sumatra, Indonesia, during 1–3 October 2013. Here each subplot between (a) and (e) in each day represents the radar maps for different elevation and azimuth angles. On the top of each figure, the elevation and azimuth angles are given. SNR = signal-to-noise ratio. Note that x axis scale in the bottom of each panel is in local time, while universal time is mentioned in the top.

(or fixed electron densities). For comparison, we have also plotted the IMF Bz variations (red plot) along with EEJ strength in Figure 5d. From the figure, it can be said that unlike quiet time variations, as time progresses, EEJ strength on this day showed large variations with EEJ/CEJ fluctuations. At one time, EEJ strength reached as high as 150 nT, which is significantly high as compared to quiet day EEJ strength. Similarly, temporal variation of virtual height on this day over TIR/HYD/ALD suggests that it reflects the variations of EEJ strength. There is a strong F_3 layer generation at 03:00–03:30 UT (08:30–09:00 IST), 05:30–06:00 UT (10:30–11:00 IST), and 10:20–13:30 UT (15:50–19:00 IST) when simultaneous rise of both EEJ strength and virtual height is noticed. It is interesting to note that virtual height went up high simultaneously at all the stations when we see such an abrupt increase in EEJ strength. It may be noted that when F_3 layers are noticed in the ionograms, rise in the virtual height especially in the higher frequency bands, namely, 8–10 MHz, is also prominently observed in the figure. This is also apparent in the evening PRE times. It may be noticed that there is a small shift (nearly 15 min) in the time of height rise at ALD in comparison to other two stations, which could be attributed to 15 min sampling interval at ALD in comparison to TIR/HYD where it is 10 min interval but it is not related to any other physical process. It is known that primary zonal electric field is in the eastward direction (usually related to EEJ currents) during daytime that pushes the F layer to higher altitudes due to upward $E \times B$ drift. However, when westward electric field dominates during daytime (usually related to CEJ currents), it can produce downward $E \times B$ drift. Since the variations in both the EEJ strength and the virtual height are very well associated with IMF Bz variations

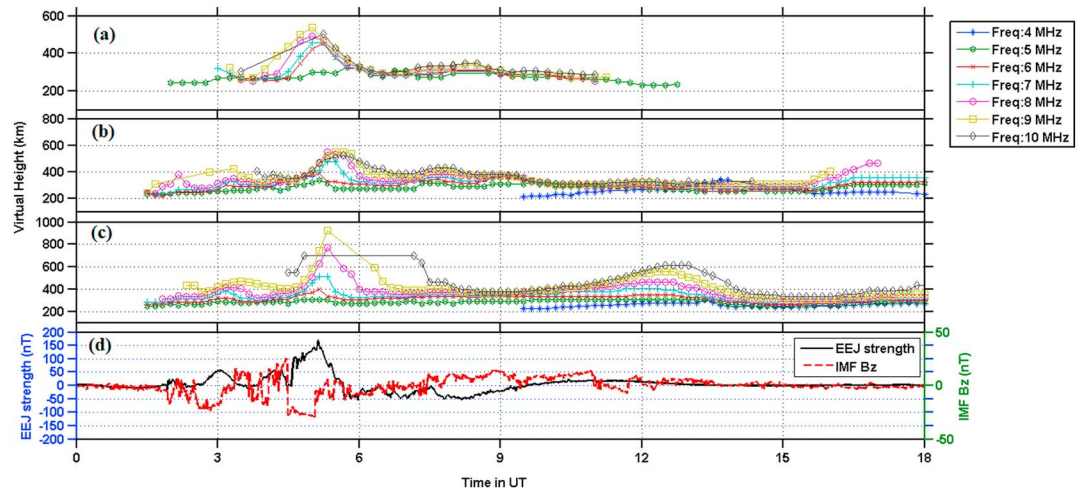


Figure 5. The virtual height variations using isodensity scaling at 5–10 MHz over (a) Allahabad (ALD), (b) Hyderabad (HYD), and (c) Tirunelveli (TIR), respectively, during 00:00–18:00 UT on 2 October 2013. Also plotted in the bottom of the figure is the equatorial electrojet (EEJ) strength (blue) and interplanetary magnetic field (IMF) Bz (red) for comparison.

(see the red plot Figure 5d) during main phase of the storm, it can be suggested that additional eastward and westward electric fields could have been imposed due to undershielding and overshielding conditions that arise from the orientation of the IMF Bz either southward or northward during the storm period. Since the storm main phase is ended by noon in Indian sector, the afternoon variations are not associated with IMF Bz variations but rather possibly related to disturbance electric fields or disturbance winds, which can impose a westward electric fields to the existing eastward electric field in the daytime to evening hour.

It is known that equatorial E_{s-q} layers disappear during geomagnetic storms whenever CEJ is observed. But Abdu, MacDougall, et al. (2003) have suggested that low-latitude E_s layers are enhanced during downward electric fields such as CEJ events. It may be mentioned that since Hyderabad ionosonde station is in low latitude, field line connection of E region over Hyderabad shall have apex altitude of ~ 280 km over magnetic equator. Figure 6 shows the temporal variations of top frequency ($f_t E_s$) of low-latitude E_s layers over Hyderabad during few quiet days as well as storm day during 00:00–15:00 UT to understand the differences between quiet and storm time E_s layer. In the figure, red indicates storm day E_s layer frequency while blue indicates quiet day E_s layer frequency. These quiet days are obtained during 25 September 2013 to 1

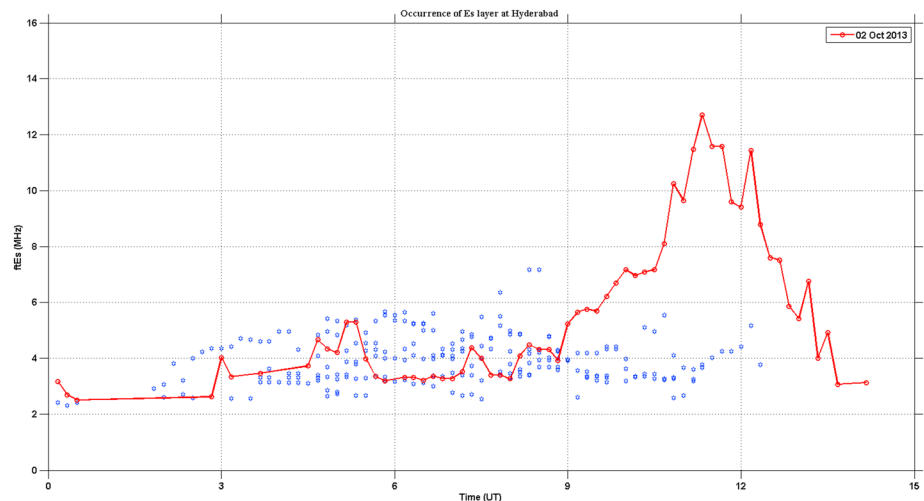


Figure 6. The temporal variation of top frequency ($f_t E_s$) of low-latitude E_s layers over Hyderabad during few quiet days (blue) and on 2 October 2013 (red) during 00:00–15:00 UT.

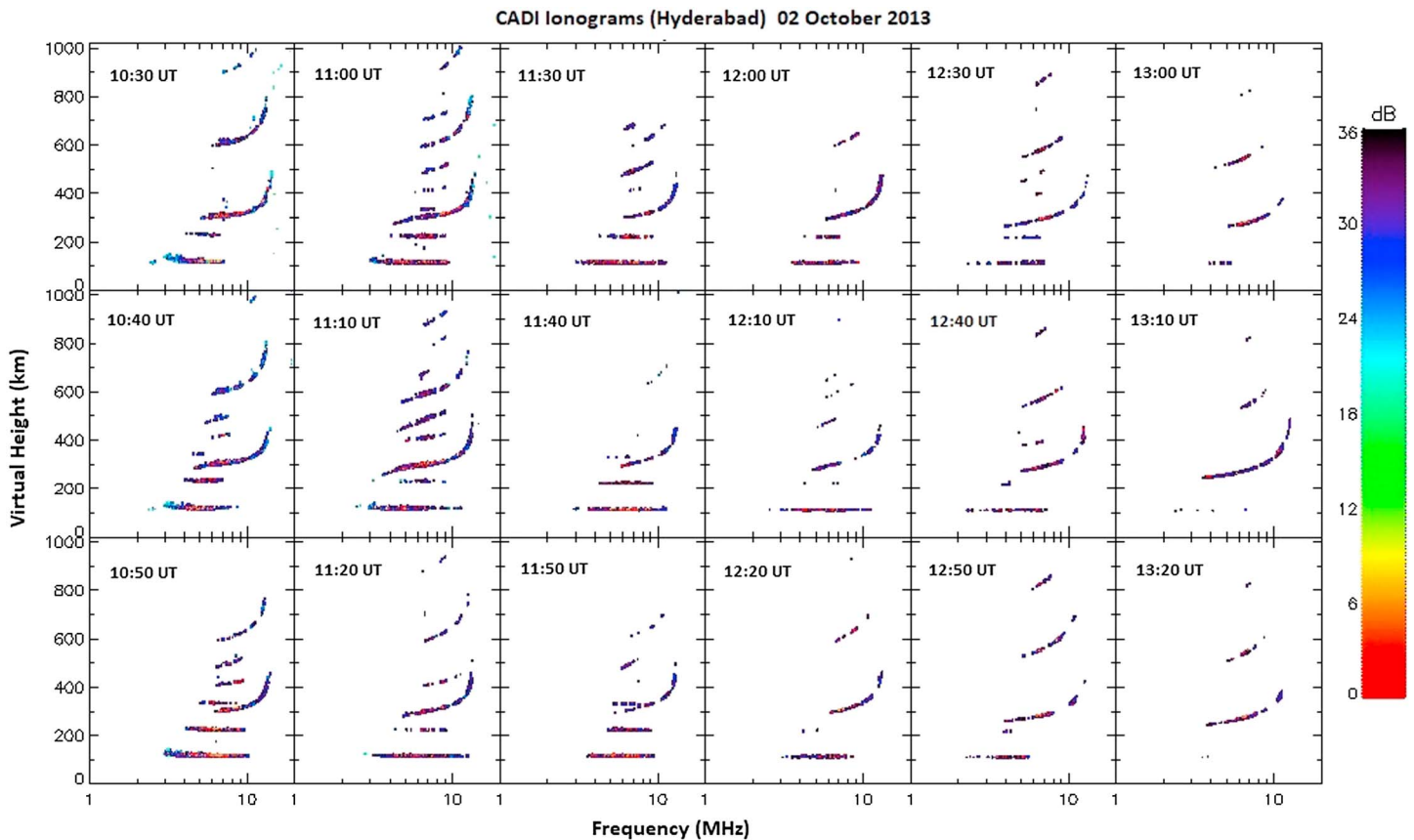


Figure 7. The ionogram images of E_s layers at Hyderabad, a low-latitude station during 10:30–13:20 UT in the evening hours on 2 October 2013. CADI = Canadian Advanced Digital Ionosonde.

October 2013, which is before the commencement of the storm days. The $f_t E_s$ observations reveal that while E_s layers during both storm day and quiet days are steadily varied up to 08:30 UT (14:00 IST), however, $f_t E_s$ values increased to as high as 12.5 MHz at 11:45 UT (17:15 IST) on storm day, which continued until 13:00 UT (18:30 IST) and then slowly decreased to reach quiet day values at 13:30 UT. The observations suggest that while E_s layers are very strong around evening hours on 2 October 2013 (storm day), they are found to be very weak on quiet days. To show the actual ionogram images, ionogram maps at different times are presented in Figure 7 during the evening hours on 2 October 2013 over Hyderabad, a low-latitude station. From both the figures, it can be stated that low-latitude E_s layer density is very high at the evening PRE time on the storm day but the density of the E_s layers is very less on other quiet days. It may be noted that the E_s layers at low latitudes are produced by both zonal winds and wind shears and vertical hall electric fields (Abdu, MacDougall, et al., 2003). So the E_s layers at Hyderabad are generated by winds and wind shears in addition to zonal electric fields. Accordingly, our strong E_s layers after 09 UT when EEJ strength is weak but not at 03 and 05 UT when EEJ strength is strong is possibly related to the competing influence of winds and electric fields. The resultant action will be decided by the strength of these two. Figure 8 shows the ionogram images of presence of F_3 layer at different times during evening hours, that is, 17:00–18:50 IST (11:30–13:20 UT) over Tirunelveli on 2 October 2013. Based on these figures, some interesting observations on the storm day can be noticed which can be stated as (a) simultaneous occurrence of F_3 layers during dusk sector and reduction of evening hour F layer height which is representative of PRE vertical drifts and (b) enhancement of E_s layers over Hyderabad station.

Figures 9a–9c show the temporal and latitudinal variation of GPS TEC maps over Indian longitude (at 80°E) as obtained from international GPS stations on these 3 days using the hourly mean TEC values. These TEC maps are produced after utilizing global TEC data and by applying spherical harmonic filtering. Here x axis shows

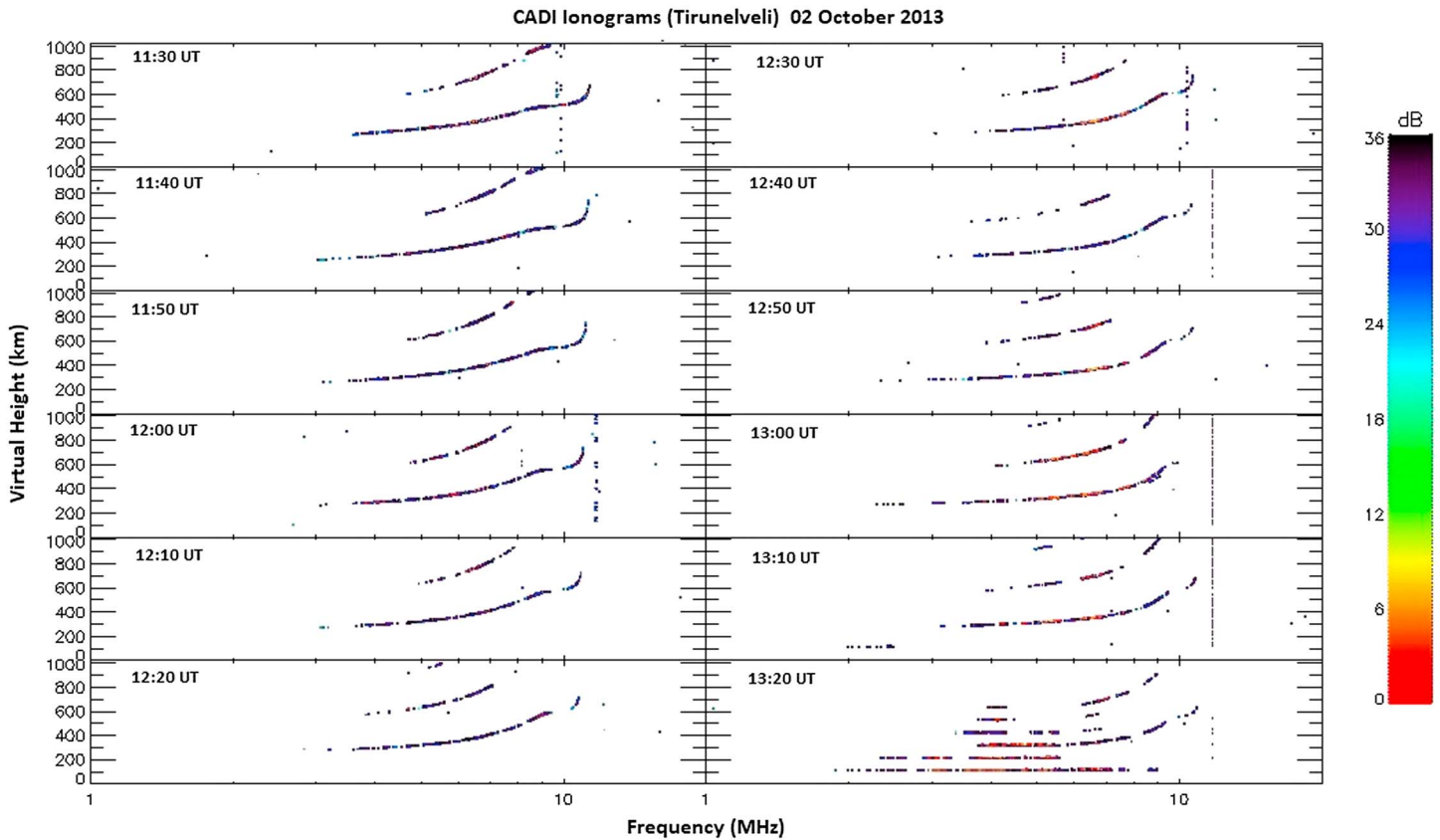


Figure 8. The ionogram images of F_3 layers at 11:30–13:20 UT during evening hours (i.e., 17:00–18:50 IST) over Tirunelveli on 2 October 2013. CADI = Canadian Advanced Digital Ionosonde.

the latitude (geographic), while y axis represents the time in UT. It is evident from the above observations that while equatorial ionization anomaly (EIA) crest is asymmetric on 2 October, it is symmetric on other two quiet days. It is known that symmetric or asymmetric EIA crests about the magnetic equator can lead to the generation or suppression of plasma bubbles depending upon the changes in the field line-integrated conductivity either through transequatorial winds or enhancing low-latitude E_s layers. It is known that the Joule heating that is generated due to auroral currents during geomagnetic storm produces equatorward meridional winds at the low latitudes. These winds in turn cause EIA asymmetry. Since we observed simultaneously strong E_s layers at low latitude, F_3 layers, and suppression of equatorial plasma irregularities on storm day across sunset terminator during “spread F ” season but not on quiet days, we believe that this storm produced quite significant electrodynamic disturbances in the low latitudes over Indian sector.

4. Discussions

From the observations, the following points mainly arise: (a) occurrence of EPBs during quiet days but suppression of EPBs during storm day during “spread F season,” (b) simultaneous presence of F_3 layers at both equatorial and low-latitude stations in association with sudden increase of EEJ strength, (c) observations of intense blanketing E_s layers at low latitude during the time of PRE on the storm day but weak/absence of E_s layers during quiet days, (d) TEC maps suggesting the EIA crest symmetry during quiet days but asymmetry on storm day, and (e) simultaneous suppression of EPBs and occurrence of F_3 layer during sunset period. From the observations, it is obvious that during the main phase of the storm, several episodes of sudden increase/decrease of EEJ strength are evident. On one occasion, EEJ went up to as high as 150 nT when F_3 layers are produced at all three ionosonde stations indicating that there exists a common driver for these two processes. It is believed that vertical $E \times B$ drift is the common driver for both processes. The increase

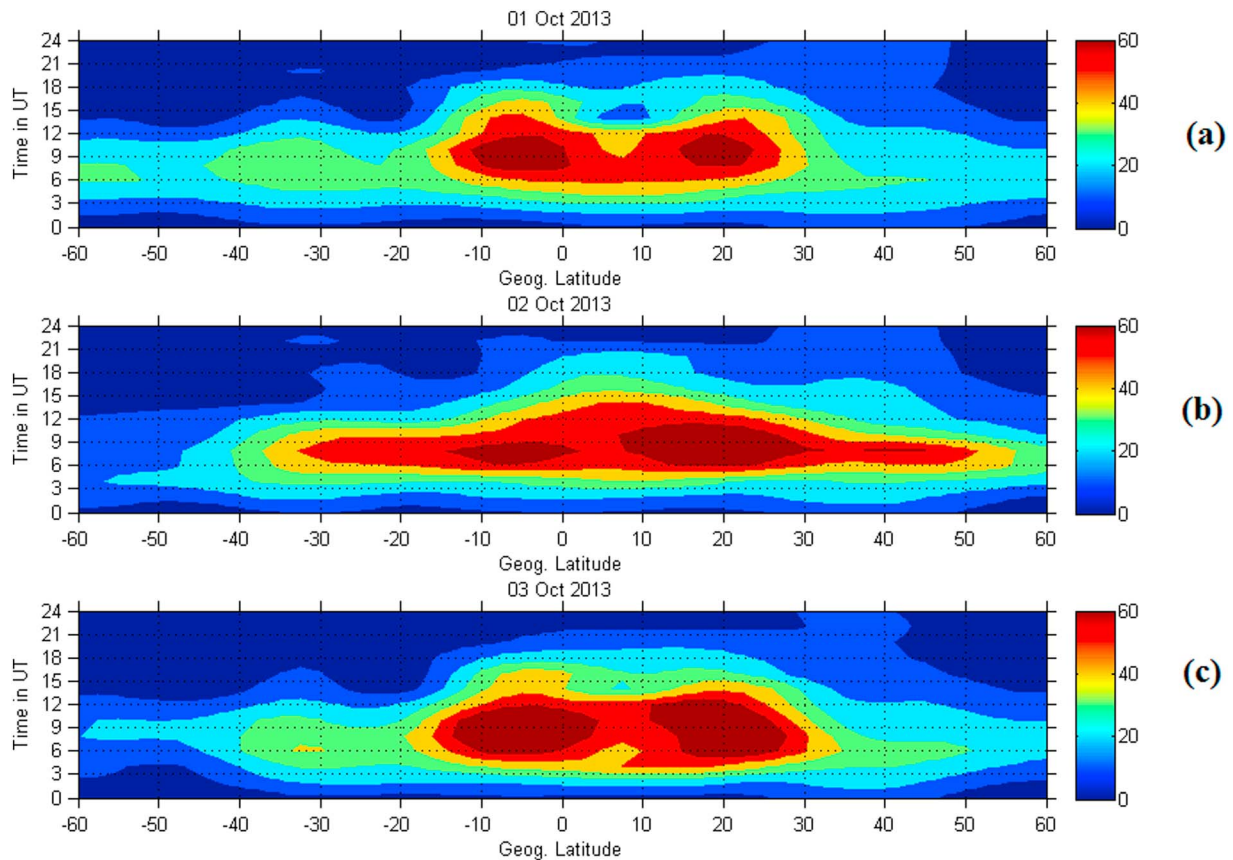


Figure 9. (a–c) The temporal and latitudinal variation of total electron content maps over Indian longitude (80°E) as obtained using the data from international Global Positioning System stations during 1–3 October 2013.

and decrease of EEJ strength are directly associated with the undershielding and overshielding conditions of the eastward/westward electric fields during daytime due to the southward/northward turning of the IMF B_z . During this storm event, main phase is observed in the daytime over Indian sector but recovery started from 06:00 UT (11:30 IST) and it continued until the next day. During recovery phase, even though EPBs were suppressed, F_3 layers were present at the evening hours over Indian sector, which is not a regular phenomenon. Since F_3 layers are generated under the combined action of upward vertical $E \times B$ drift and equatorward meridional winds during daytime, presence of downward drift during evening PRE times on the storm day raises questions over its source mechanism. Though many reports have showed the generation or suppression of EPBs, no report is available on the simultaneous suppression of EPBs and presence of F_3 layers around the sunset terminator.

It may be mentioned that Sreeja et al. (2009) have studied the occurrence of F_3 layers over equatorial station, Trivandrum during geomagnetic storms in the dawn and dusk sectors. They suggested that occurrence of F_3 layers is caused mainly by imposition of additional eastward electric field due to undershielding condition under the southward IMF B_z condition. However, by the time storm recovery started in our case, it is local noon hours in Indian sector. By then, onset time of the storm is beyond 3 h. So there is no question of magnetospheric electric fields impacting the evening hours over Indian sector either through changes in the IMF B_z or in the AE index. Hence, all the results in the evening sector point at the DDEFs or disturbance winds that can influence the equatorial and low-latitude ionosphere on 2 October 2013. We have seen that the AE index had double peaked structure in its strength during main phase of the storm (before noon), which is representative of Joule heating. This could produce equatorward surge of thermospheric meridional neutral winds and traveling ionospheric disturbances. Accordingly, disturbance winds and traveling ionospheric disturbances could become intense during evening or late night of 2 October 2013 depending upon their

propagation speeds. Thermospheric neutral wind circulations produced by auroral Joule heating during geomagnetic storms at high latitudes are investigated using numerical simulations (Blanc & Richmond, 1980). According to them, due to auroral Joule heating, equatorward winds blow above ~ 120 km at midlatitudes through Hadley circulation cell. However, due to Coriolis effect of the Earth's rotation, these winds turn westward in the midlatitudes. Accordingly, these westward disturbance winds at midlatitudes drive equatorward Pedersen currents, which accumulate the charges toward the equator, resulting in the generation of a poleward electric field, a westward plasma drift and an eastward Hall current. This eastward midlatitude Hall current closes circuit partly via lower latitudes resulting in an "anti-Sq" type of current vortex, when realistic local time conductivity variations are considered. Due to this, opposite polarity of electric fields and reverse currents are produced at low latitudes that oppose the normal quiet time behavior. When this is superimposed on to the background quiet time pattern, their behavior is quite different. These electric field perturbations are "westward" during the day and evening but "eastward" during the midnight to early morning hours but have larger amplitudes near the dawn and dusk terminators.

Drastic increase of the electron density over the equator during evening hours on 2 October 2013 than on quiet days suggests that DDEFs are indeed westward to produce vertically downward Hall electric fields. Even the ionosonde height variations on 2 October 2013 also suggest that vertical drifts are downward. Now it is believed that since evening PRE drifts are known to be caused by the combination of thermospheric eastward zonal winds and longitudinal/local time gradient in the E layer conductivity, which in turn depend on storm time electrodynamics, the variability in these parameters may be playing significant role in the generation of plasma irregularities. Also, the anomalous generation of blanketing E_s layers at low latitude in the storm day may be associated with storm time disturbance winds/electric fields. As electric fields and winds are significantly modified during geomagnetic storm, it will have impact on low-latitude E and F region coupling and hence accordingly affects the low-latitude electrodynamics and generation of E_s layers and plasma irregularities (Abdu, MacDougall, et al., 2003). Stephan et al. (2002) have examined the variations in the flux tube-integrated Pedersen conductivities of E and F regions in the dusk sector by altering the sporadic E layer density at low latitudes and its role in the ESF development. They found that the growth rate of RT instability to be lowered by 1 order less when sporadic E layer density of the order of 10^6 cm³ in the height range of 115–120 km is considered. Accordingly, they suggested that small increase in the postsunset E region density could lead to the reduction in the upward plasma drift of the PRE, which is a key parameter in the growth rate of the ESF instability and could cause the suppression of EPBs. Our observations of strong E_s layer density with f_1E_s of 12 MHz, that is, 1.7×10^6 cm³, are of the same order as that mentioned by Stephan et al. (2002). Similarly, Abdu, MacDougall, et al. (2003) have investigated the evening PRE and its relation to sporadic E layer formation in the evening hours over Fortaleza, a low-latitude station in the Brazil. Their results also suggest that larger PRE amplitudes are found to disrupt the E_s layer; however, no disruption occurs under smaller PRE amplitudes. Also, no E_s layer disruption occurs when PRE amplitude decreases or is inhibited under DDEFs. Recently Joshi, Patra, Pant, and Rao (2013) have investigated the possible connection between low-latitude E_s layers and EPBs during geomagnetically quiet days over Indian sector. Their results also indicate that when blanketing type E_s occurs at low latitudes for long duration in the sunset hours, significant rise in PRE height is not observed resulting in absence of EPBs. In contrast, when no E_s or nonblanketing type E_s is present, PRE height went up high and EPBs are observed. But strong E_s layers as seen in our case may affect the EPBs since the association between the amplitude of PRE and E_s layer disruption/formation could be related to the storm time E and F region coupling process under the development of vertical Hall electric field around the sunset terminator (e.g., Abdu, MacDougall, et al., 2003).

Carrasco et al. (2007) have investigated the role of vertical Hall electric field in suppressing or enhancing the E_s layers using numerical simulations in the Brazilian sector during quiet days. They suggested that while an upward vertical electric field is capable of disrupting an ongoing sporadic E layer, whereas a downward electric field favors its formation. Accordingly, downward drift in the present case may be responsible for the formation of strong sporadic E_s layers at Hyderabad station. Further, Abdu et al. (2009) have suggested that vertical Hall electric field induced by the primary zonal electric field during the storm can enhance the field line-integrated conductivity ratio of Hall to Pedersen and can cause either convergence or divergence of the ionization leading to the E_s layer formation or disruption. Accordingly, downward polarity of Hall electric field can cause E_s layer formation; however, upward polarity of Hall electric field can cause E_s layer disruption.

It may be mentioned that while many reports are available on the low-latitude E_s layers affecting the ESF generation or suppression in the Brazilian longitudes, very few observations are available in Indian longitude. Using low-latitude ionosonde, Joshi, Patra, and Rao (2013) have investigated the effect of evening low-latitude E_s layer activity on the occurrence of ESF over India. Their results also suggest that the development of EPBs depends very much on the height and type of low-latitude E_s layer. They suggested that depending upon the height of the E_s layer, it can either suppress or enhance the ESF activity over Indian longitude. However, they did not investigate the role of E_s layers in ESF during geomagnetic storms. Since $h'F$ (km) of the F layer over TIR is hovering at <300 km altitude in our case during the storm day, we believe that strong presence of blanketing E_s layers in the evening hours at Hyderabad is also having a role in EPB suppression. It is known that the F region electric field in the evening sector is eastward, corresponding to an upward PRE. However, a strong E_s layer at low latitude will cause a decrease in the upward PRE and the growth rate of the RT instability, resulting in suppression of EPB occurrence. As, in the present case, the vertical plasma drift at 12–14 UT (near the PRE time) is downward (Figure 2c), corresponding to a westward electric field and hence, existence of a strong E_s layer at low-latitude station may reduce the strength of the westward electric field and reduce the downward plasma drift. Accordingly, presence of strong E_s layers may also be to weaken the EPB suppression, if already downward drift exists. Even the electron density of the E_{sb} on storm day (as shown in Figure 6) is significantly higher than on quiet days. But the presence of F_3 layer when EPBs are suppressed is not consistent with our understanding. It appears that storm time winds and/or electro-dynamics of E and F regions along the sunset terminator may be responsible for these peculiar results.

It is known that, during equinoxes, uplift of the ionosphere near the magnetic equator by an eastward electric field in the afternoon reduces ion drag on the neutral wind that results in strong eastward winds in the evening hours that is conducive for the EPB development (e.g., Richmond et al., 1992). However, since we have observed strong densities in the F region near the equator and asymmetric EIA crests on the storm day (see TEC map in Figure 9) due to absence of upward drift in association with the CEJ currents and disturbance winds or electric fields in the afternoon, there is a possibility that it can produce large ion drag on the neutrals during evening hours that ultimately can reduce or reverse the zonal winds. This can ultimately produce downward Hall electric field, which can enhance the E_s layers at low latitudes. These E_s layers can further increase the field-integrated conductivities to suppress the EPBs. While this appears to be plausible reason for the suppression of EPBs, simultaneous presence of F_3 layers negates this hypothesis. Balan and Bailey (1995) have suggested that F_3 layers over low latitudes could be generated through the combination of eastward electric fields in the presence of equatorward meridional winds. However, Balan et al. (2008) have later suggested that the F_3 layers can also be produced in the local evening when unusual large downward $E \times B$ drifts are seen. But their result does not indicate that simultaneously EPBs can be suppressed. Since disturbance winds and DD seem to be significantly active in the evening sector on 2 October 2013 over Indian sector, it is possible that F_3 layers that are seen here could be generated by the combination of equatorward meridional winds with the altitude variation of downward drifts. This is only a possibility that our observations of suppression of EPBs and F_3 layers support that such physical process may exist. Alternately, if the altitude/latitude variation of the vertical Hall polarization electric field can have upward or downward drifts around sunset as it appears to be true in the present case, that also can cause simultaneous occurrence of F_3 layers, E_s layer formation, and suppression of EPBs through the changes in the conductivity profiles. Hence, it appears that while the altitude/latitude variation of storm time electro-dynamical coupling processes between the E and F regions could be linked to such unique observations, still we need more analysis to improve upon.

5. Conclusions

Here we studied the storm time electro-dynamical response of the equatorial and low-latitude ionosphere to a moderate geomagnetic storm that occurred on 2 October 2013 where Dst reached -80 nT using a chain of ionosondes over Indian longitude along with a GPS receiver located at Tirunelveli. The results show that even a moderate geomagnetic storm can play a significant role in the day-to-day variability of the EPBs. The main findings of the present study can be summarized as follows:

1. Observed simultaneous enhancement of EEJ strength and presence of F_3 layers in all ionosondes from equator to low latitudes during overshielding electric fields in the day.

2. Observed occurrence of EPBs on quiet days when F layer is lifted up but suppression of postsunset EPBs when F layer is pushed down on storm day during equinoctial month.
3. Observations of intense E_s layers at low latitudes at the time of evening PRE development on storm day but weak E_s layers on quiet days.
4. Simultaneous presence of F_3 layers, suppression of EPBs over Tirunelveli, an equatorial station around sunset times but intense occurrence of E_s layers at Hyderabad may suggest possible E and F region coupling during this storm.
5. GPS TEC maps suggest strong EIA crest symmetry on quiet days but asymmetry on storm day, which may be due to DDEF/disturbance winds.
6. The association of strong EIA asymmetry on storm day suggesting storm associated transequatorial meridional wind flow.
7. The results suggest that the altitude/latitude variation of E and F regions linked with DDEFs/disturbed winds might be responsible for the simultaneous detection of F_3 layers, occurrence of intense low-latitude E_s layers, and suppression of EPBs along the sunset terminator.

Acknowledgments

The research work presented here is carried out through the funds from the in-house project at IIG (DST), Government of India. Part of this work is carried out at ICTP, Italy, where one of the authors (S. S.) visit under its associateship program. S. S. also would like to thank the Director, IIG for his support and guidance. We would like to acknowledge Prabhakar Tiwari at KSKGRL, Allahabad, for his support in maintaining the CADI at Allahabad. Solar and interplanetary data are obtained from <http://omniweb.gsfc.nasa.gov/in/>, while SYM-H data are obtained from WDC, Kyoto, Japan. We also acknowledge the use of EAR maps that are obtained from EAR website. All the data sets presented in this paper are with the corresponding author and his email is ssrpathi.iig@gmail.com.

References

- Aarons, J. (1991). The role of the ring current in the generation or inhibition of equatorial F layer irregularities during magnetic storms. *Radio Science*, 26(4), 1131–1149. <https://doi.org/10.1029/91RS00473>
- Abdu, M. A. (1997). Major phenomena of the equatorial ionosphere-thermosphere system under disturbed conditions. *Journal of Atmospheric and Solar - Terrestrial Physics*, 59(13), 1505–1519. [https://doi.org/10.1016/S1364-6826\(96\)00152-6](https://doi.org/10.1016/S1364-6826(96)00152-6)
- Abdu, M. A., Batista, I. S., Takahashi, H., MacDougall, J., Sobral, J. H., Medeiros, A. F., & Trivedi, N. B. (2003). Magnetospheric disturbance induced equatorial plasma bubble development and dynamics: A case study in Brazilian sector. *Journal of Geophysical Research*, 108(A12), 1449. <https://doi.org/10.1029/2002JA009721>
- Abdu, M. A., Batista, I. S., Walker, G. O., Sobral, J. H. A., Trivedi, N. B., & de Paula, E. R. (1995). Equatorial ionospheric electric fields during magnetospheric disturbances: Local time/longitude dependences from recent EITS campaigns. *Journal of Atmospheric and Terrestrial Physics*, 57(10), 1065–1083.
- Abdu, M. A., de Souza, J. R., Batista, I. S., Santos, A. M., Sobral, J. H. A., Rastogi, R. G., & Chandra, H. (2014). The role of electric fields in sporadic E layer formation over low latitudes under quiet and magnetic storm conditions. *Journal of Atmospheric and Solar - Terrestrial Physics*, 115(2014), 95–105.
- Abdu, M. A., Kherani, E. A., Batista, I. S., & Sobral, J. H. A. (2009). Equatorial evening prereversal vertical drift and spread F suppression by disturbance penetration electric fields. *Geophysical Research Letters*, 36, L19103. <https://doi.org/10.1029/2009GL039919>
- Abdu, M. A., MacDougall, J. W., Batista, I. S., Sobral, J. H. A., & Jayachandran, P. T. (2003). Equatorial evening prereversal electric field enhancement and sporadic E layer disruption: A manifestation of E and F region coupling. *Journal of Geophysical Research*, 108(A6), 1254. <https://doi.org/10.1029/2002JA009285>
- Abdu, M. A., Sastri, J. H., Luhr, H., Tachihara, H., Kitamura, T., Trivedi, N. B., & Sobral, J. H. A. (1998). DP 2 electric field fluctuations in the dusk-time dip equatorial ionosphere. *Geophysical Research Letters*, 25(9), 1511–1514. <https://doi.org/10.1029/98GL01096>
- Abdu, M. A., Souza, J. R., Batista, I. S., Fejer, B. G., & Sobral, J. H. A. (2013). Sporadic E layer development and disruption at low latitudes by prompt penetration electric fields during magnetic storms. *Journal of Geophysical Research: Space Physics*, 118, 2639–2647. <https://doi.org/10.1002/jgra.50271>
- Alex, S., & Rastogi, R. (1986). Geomagnetic disturbance effect on equatorial spread- F . *Annales de Geophysique*, 5A, 83.
- Balan, N., & Bailey, G. J. (1995). Equatorial plasma fountain and its effects: Possibility of an additional layer. *Journal of Geophysical Research*, 100, 2047.
- Balan, N., Thampi, S. V., Lynn, K., Otsuka, Y., Alleyne, H., Watanabe, S., et al. (2008). F_3 layer during penetration electric field. *Journal of Geophysical Research*, 113, A00A07. <https://doi.org/10.1029/2008JA013206>
- Becker-Guedes, F., Sahai, Y., Fagundes, P. R., Lima, W. L. C., Pillat, V. G., Abalde, R., & Bittencourt, J. A. (2004). Geomagnetic storm and equatorial spread- F . *Annales de Geophysique*, 22(9), 3231–3239. <https://doi.org/10.5194/angeo-22-3231-2004>
- Bhattacharyya, A. (2004). Role of E region conductivity in the development of equatorial ionospheric plasma bubbles. *Geophysical Research Letters*, 31, L06806. <https://doi.org/10.1029/2003GL018960>
- Blanc, M., & Richmond, A. D. (1980). The ionospheric disturbance dynamo. *Journal of Geophysical Research*, 85, 1669–1686.
- Carrasco, A. J., Batista, I. S., & Abdu, M. A. (2007). Simulation of the sporadic E layer response to prereversal associated evening vertical electric field enhancement near dip equator. *Journal of Geophysical Research*, 112, A06324. <https://doi.org/10.1029/2006JA012143>
- Chandra, H., & Rastogi, R. G. (1974). Geomagnetic storm effects on ionospheric drifts and the equatorial E_s over the magnetic equator. *Indian Journal of Radio & Space Physics*, 3, 332–336.
- Dabas, R. S., Lakshmi, D. R., & Reddy, B. M. (1989). Effect of geomagnetic disturbances on VHF nighttime scintillation activity at equatorial and low latitudes. *Radio Science*, 4, 563–573.
- DasGupta, A., Maitra, A., & Das, S. K. (1985). Postmidnight equatorial scintillation activity in relation to geomagnetic disturbances. *Journal of Atmospheric and Terrestrial Physics*, 47(8–10), 911–916. [https://doi.org/10.1016/0021-9169\(85\)90067-4](https://doi.org/10.1016/0021-9169(85)90067-4)
- Fejer, B. G. (1997). The electrodynamics of the low-latitude ionosphere: Recent results and future challenges. *Journal of Atmospheric and Solar - Terrestrial Physics*, 59(13), 1465–1482. [https://doi.org/10.1016/S1364-6826\(96\)00149-6](https://doi.org/10.1016/S1364-6826(96)00149-6)
- Fejer, B. G., & Kelley, M. C. (1980). Ionospheric irregularities. *Reviews of Geophysics and Space Physics*, 18(2), 401. <https://doi.org/10.1029/RG018i002p00401>
- Fukao, S., Ozawa, Y., Yokoyama, T., Yamamoto, M., & Tsunoda, R. T. (2004). First observations of spatial structures of F region 3-m-scale field-aligned irregularities with the Equatorial Atmosphere Radar in Indonesia. *Journal of Geophysical Research*, 109, A02304. <https://doi.org/10.1029/2003JA010096>
- Gonzalez, W. D., Joselyn, J. A., Kamide, Y., Kroehl, H. W., Rostoker, G., Tsurutani, B. T., & Vasyliunas, V. M. (1994). What is a geomagnetic storm? *Journal of Geophysical Research*, 99(A4), 5771–5792.

- Huang, C., Burke, W., Machuzak, J., Gentile, L., & Sultan, P. (2002). Equatorial plasma bubbles observed by DMSP satellites during a full solar cycle: Toward a global climatology. *Journal of Geophysical Research*, *107*(A12), 1434. <https://doi.org/10.1029/2002JA009452>
- Huang, C.-S., Foster, J. C., & Kelley, M. C. (2005). Long-duration penetration of the interplanetary electric field to the low-latitude ionosphere during the main phase of magnetic storms. *Journal of Geophysical Research*, *110*, A11309. <https://doi.org/10.1029/2005JA011202>
- Joshi, L. M., Patra, A. K., Pant, T. K., & Rao, S. V. B. (2013). On the nature of low-latitude E_s influencing the genesis of equatorial plasma bubble. *Journal of Geophysical Research: Space Physics*, *118*, 524–532. <https://doi.org/10.1029/2012JA018122>
- Joshi, L. M., Patra, A. K., & Rao, S. V. B. (2013). Low-latitude E_s capable of controlling the onset of equatorial spread F . *Journal of Geophysical Research: Space Physics*, *118*, 1170–1179. <https://doi.org/10.1002/jgra.50189>
- Kelley, M. C., Fejer, B. G., & Gonzalez, C. A. (1979). An explanation for anomalous equatorial ionospheric electric fields associated with the northward turning of the interplanetary magnetic field. *Geophysical Research Letters*, *6*(4), 301–304. <https://doi.org/10.1029/GL006i004p00301>
- Kikuchi, T. H., Luehr, T., Kitamura, O. S., & Schlegel, K. (1996). Direct penetration of the polar electric field to the equator during a DP2 event as detected by the auroral and equatorial magnetometer chains and the EISCAT radar. *Journal of Geophysical Research*, *101*(A8), 17,161–17,173. <https://doi.org/10.1029/96JA01299>
- Lee, C. C., Liu, J. Y., Reinisch, B. W., Lee, Y. P., & Liu, L. (2002). The propagation of traveling atmospheric disturbances observed during the April 6–7, 2000 ionospheric storm. *Geophysical Research Letters*, *29*(5), 1068. <https://doi.org/10.1029/2001GL013516>
- Lei, J., Burns, A. G., Tsugawa, T., Wang, W., Solomon, S. C., & Wiltberger, M. (2008). Observations and simulations of quasiperiodic ionospheric oscillations and large-scale traveling disturbances during the December 2006 geomagnetic storm. *Journal of Geophysical Research*, *113*, A06310. <https://doi.org/10.1029/2008JA013090>
- Lei, J., Zhong, J., Mao, T., Hu, L., Yu, T., Luan, X., et al. (2016). Contrasting behavior of the F_2 peak and the topside ionosphere in response to the 2 October 2013 geomagnetic storm. *Journal of Geophysical Research: Space Physics*, *121*, 10,549–10,563. <https://doi.org/10.1002/2016JA022959>
- Mao, T., Sun, L., Hu, L., Wang, Y., & Wang, Z. (2015). A case study of ionospheric storm effects in the Chinese sector during the October 2013 geomagnetic storm. *Advances in Space Research*, *56*(9), 2030–2039. <https://doi.org/10.1016/j.asr.2015.05.045>
- Martinis, C. R., Mendillo, M. J., & Aarons, J. (2005). Toward a synthesis of equatorial spread F onset and suppression during geomagnetic storms. *Journal of Geophysical Research*, *110*, A07306. <https://doi.org/10.1029/2003JA010362>
- Nava, B., Rodríguez-Zuluaga, J., Alazo-Cuartas, K., Kashcheyev, A., Migoya-Orué, Y., Radicella, S. M., et al. (2016). Middle- and low-latitude ionosphere response to 2015 St. Patrick's Day geomagnetic storm. *Journal of Geophysical Research: Space Physics*, *121*, 3421–3438. <https://doi.org/10.1002/2015JA022299>
- Ramsingh, S., Sripathi, S., Sree Kumar, S., Banola, K., Emperumal, P. T., & Kumar, B. S. (2015). Low-latitude ionosphere response to super geomagnetic storm of 17/18 March 2015: Results from a chain of ground-based observations over Indian sector. *Journal of Geophysical Research: Space Physics*, *120*, 10,864–10,882. <https://doi.org/10.1002/2015JA021509>
- Rastogi, R. G. (1974). Westward equatorial electrojet during daytime hours. *Journal of Geophysical Research*, *79*(10).
- Rastogi, R. G., Mullen, J. P., & McKenzie, E. (1981). Effect of magnetic activity on equatorial radio VHF scintillations and spread F . *Journal of Geophysical Research*, *86*(A5), 3661–3664. <https://doi.org/10.1029/JA086iA05p03661>
- Richmond, A. D., Ridley, E. C., & Roble, R. G. (1992). A thermosphere/ionosphere general circulation model with coupled electrodynamics. *Geophysical Research Letters*, *19*(6), 601–604. <https://doi.org/10.1029/92GL00401>
- Sastri, J. H. (1988). fields of Equatorial fields of the disturbance dynamo origin. *Annales de Geophysique*, *6*, 635.
- Sastri, J. H., Niranjan, K., & Subbarao, K. S. V. (2002). Response of the equatorial ionosphere in the Indian (midnight) sector to the severe magnetic storm of July 15, 2000. *Geophysical Research Letters*, *29*(13), 1651. <https://doi.org/10.1029/2002GL015133>
- Somayajulu, V. V., Reddy, C. A., & Viswanathan, K. S. (1987). Penetration of magnetospheric convective electric field to the equatorial ionosphere during the substorm of March 22, 1979. *Geophysical Research Letters*, *14*(8), 876–879. <https://doi.org/10.1029/GL014i008p00876>
- Sreeja, V., Balan, N., Ravindran, S., Pant, T. K., Sridharan, R., & Bailey, G. J. (2009). Additional stratifications in the equatorial F region at dawn and dusk during geomagnetic storms: Role of electrodynamics. *Journal of Geophysical Research*, *114*, A08309. <https://doi.org/10.1029/2009JA014373>
- Stephan, A. W., Colerico, M., Mendillo, M., Reinisch, B. W., & Anderson, D. (2002). Suppression of equatorial spread F by sporadic E . *Journal of Geophysical Research*, *107*(A2), 1021. <https://doi.org/10.1029/2001JA000162>
- Subbarao, K. S. V., & Murthy, B. V. K. (1994). Seasonal variations of equatorial spread- F . *Annales de Geophysique*, *12*(1), 33–39. <https://doi.org/10.1007/s00585-994-0033-4>
- Tulasi Ram, S., Rama Rao, P. V. S., Prasad, D. S. V. D., Niranjan, K., Gopi Krishna, S., Sridharan, R., & Ravindran, S. (2008). Local time dependent response of postsunset ESF during geomagnetic storms. *Journal of Geophysical Research*, *113*, A07310. <https://doi.org/10.1029/2007JA012922>